National Aeronautics and Space Administration

Characterization of Orbital Debris Photometric Properties Derived from Laboratory-Based Measurements

Heather Cowardin (ESCG), **Pat Seitzer** (University of Michigan), **Kira Abercromby** (*California Polytechnic State University*), **Ed Barker** (*LZ Technology*), **and Thomas Schildknecht** (*Astronomical Institute, University of Bern*)

Introduction

Capitalizing on optical data products and applying them to generate a more complete understanding of orbital space objects, is a key objective of NASA's Optical Measurement Program, and a primary objective for the creation of the Optical Measurements Center (OMC). The OMC attempts to emulate space-based illumination conditions using equipment and techniques that parallel telescopic observations and source-target-sensor orientations. The data acquired in the OMC are a function of known shape, size, and material. These three physical parameters are key to understanding the orbital debris environment in more depth. For optical observations, one must rely on spectroscopic or photometric measurements to ascertain an object's material type. Determination of an object's shape using remote observations is more complicated due to the various light scattering properties each object presents and is a subject that requires more study. It is much easier to look at the periodicity of the lightcurve and analyze its structure for rotation.

In order to best simulate the orbital debris population, three main sources were used as test fragments for optical measurements: flight-ready materials, destructive hypervelocity testing (simulating on-orbit collisions) and destructive pressure testing (simulating on-orbit explosions). Laboratory optical characteristics of fragments were measured, including lightcurve shape, phase angle dependence, and photometric and spectroscopic color indices. These characteristics were then compared with similar optical measurements acquired from telescopic observations in order to correlate remote and laboratory properties with the intent of ascertaining the intrinsic properties of the observed orbital debris.

Laboratory Measurements

- Data acquired using the following instruments:
  - 75 watt, Xenon arc lamp to simulate the solar illumination
  - SBIG ST-8XMEI camera, with a front-side illuminated 1024 x 1536 pixels, KAF1602E Silicon CCD
  - SBIG CFW8A 5-position filter wheel that uses the standard astronomical suite of Johnson/Bessell filters
  - Analytical Spectral Device field spectrometer with a range from 300-2500 nm to baseline various material types
- Photometric measurements acquired at 6°, 36°, and 68° phase angles in 10° increments over a 360° rotation
- Following color index data limited to 6° phase angle
- Objects with poor signal in the I band will not have a respective value for the B-I color index

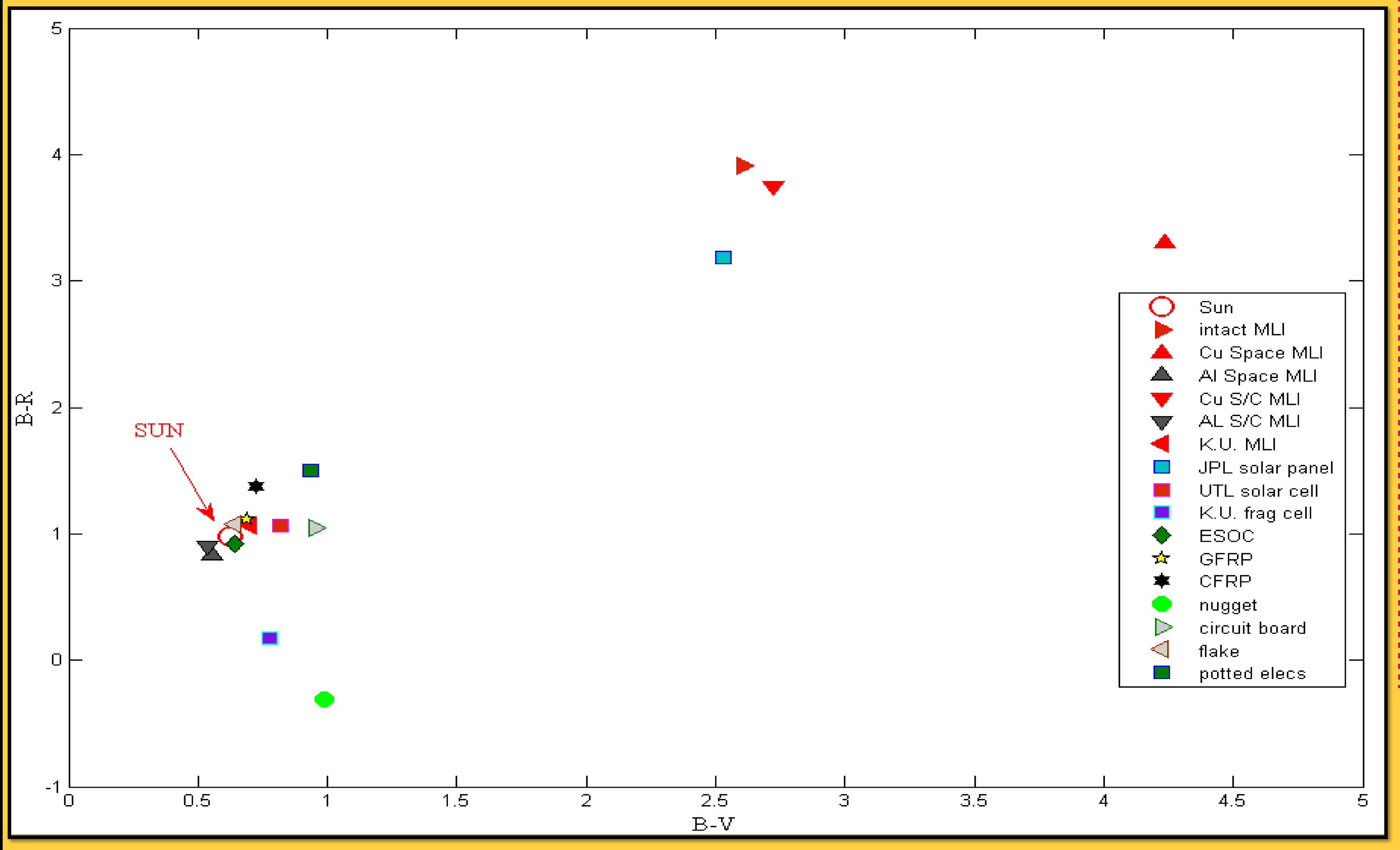

Figure 1. Photometric B-R vs. B-V color indices for all fourteen laboratory fragments.

Table 1. Laboratory samples with respective photometric color indices

Id	Material	Material	B-V	B-R	B-I
1	Intact MLI	Space-facing, spacecraft-facing	+2.0	+2.9	+2.5
2	Layer MLI: Space-facing Kapton	Copper Kapton, Aluminized Kapton	+2.3, -0.1	+3.6, -0.1	+3.6, -0.3
3	Layer MLI: Spacecraft-facing Kapton	Aluminized Kapton, Copper Kapton	-0.1, +2.1	-0.1, +2.8	-0.8, +2.8
4	Impacted MLI	Layers of copper Kapton sandwiched with Mylar and beta cloth substitute	+0.1	+0.1	-0.9
5	Solar panel	Solar cell, aluminum honeycomb interior, CFRP backing	+1.9	+2.2	+0.6
6	Intact Solar cell	Aluminized backing, solar cell	+0.2	+0.1	-2.3
7	Fragment Solar cell	Aluminum back, solar cell	+0.2	-0.8	N/A
8	Aluminum	Aluminum alloy	+0.0	-0.1	-0.8
9	Glass Fiber Reinforced Plastic	Glass fiber reinforced plastic	+0.1	+ 0.1	N/A
10	Carbon Fiber Reinforced Plastic	Carbon fiber reinforced plastic	+0.1	+0.1	N/A
11	Nugget - Potting Material	Plastic potting material	+0.4	-1.3	N/A
12	Electronic Circuit Board	Plastic back side, electronics	+0.3	+0.1	-3.0
13	Flake- Aluminum	Possible aluminum with unknown surface contaminants	+0.0	+0.1	-0.6
14	Potted Electronics	Metals and plastics	+0.3	+0.5	+0.5

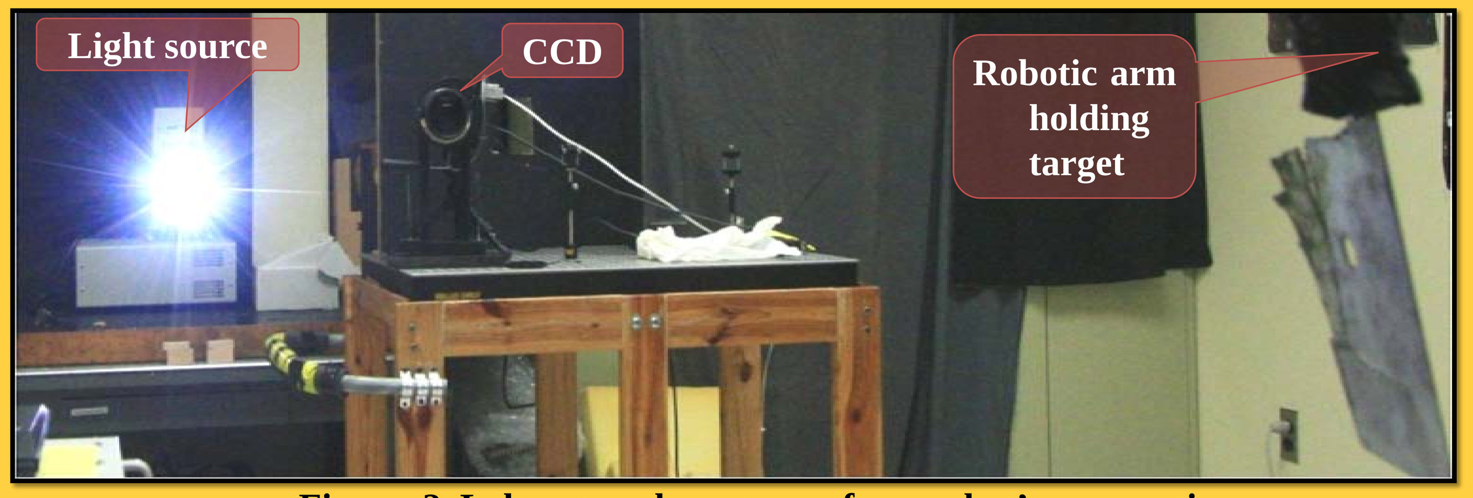

Figure 2. Laboratory layout seen from robot's perspective.

Comparison to Telescope Measurements

- The stable object (70509) shown in Fig. 3 appears to be in close proximity of the Mylar and laboratory solar panel, purely based on color index data. To make the best possible correlations between laboratory and remote data, one needs the approximate A/m for objects in Earth orbit to narrow down the large material possibilities. If the A/m of the GEO object was known, one could identify which material the object was best correlated to. If the GEO object's A/m ratio was between ~0.5 m^2/kg <A/m <1.0 m^2/kg it could be the solar panel, where as the Mylar has an A/m exceeding 30 m^2/kg.
- Fours sets of filter photometry data are shown in Fig.4 taken with CTIO 0.9 m. Object is stable on short time sequences (5-20 mins), but on longer time scales the object appears to brighten in the B and V filter, and decrease in the R and I band an approximately same time. This type of behavior is also seen in the laboratory when the copper-colored Kapton rotates toward the aluminized Kapton face with single layers of MLI. The magnitude changes from peaking in the R to peaking in the B or V, respectively.

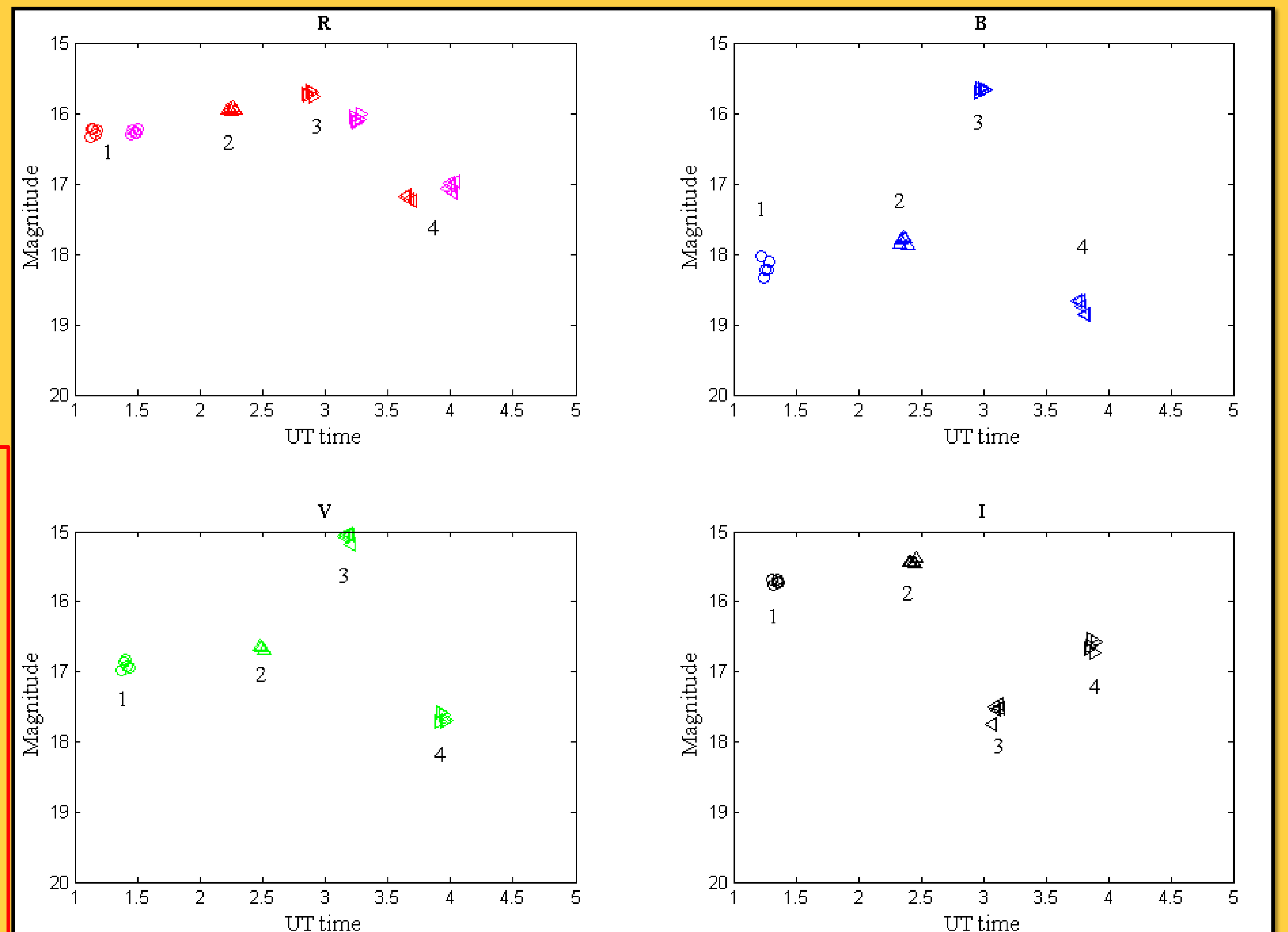

Figure 4. Four sequences of filter photometry acquired by CTIO 0.9 m on GEO object.

→ Highlights ←

- Provide color indices using laboratory photometric and spectroscopic techniques to compare with telescopic data.
- Color index data acquired using photometric and spectroscopic techniques are comparable.
- Majority of laboratory fragments had a variance over all rotations within 1σ of solar values (using photometric techniques), with exception of copper-colored Kapton material and JPL solar panel.
- Comparisons to telescope data requires a stable GEO object.
- Possible laboratory correlation to CTIO 0.9 m data, change in B-R mimics the change seen in MLI layers when the aluminized Kapton becomes illuminated.
- Future work to expand subset to include larger range of sizes, materials, and shapes to compare with photometric telescope data.

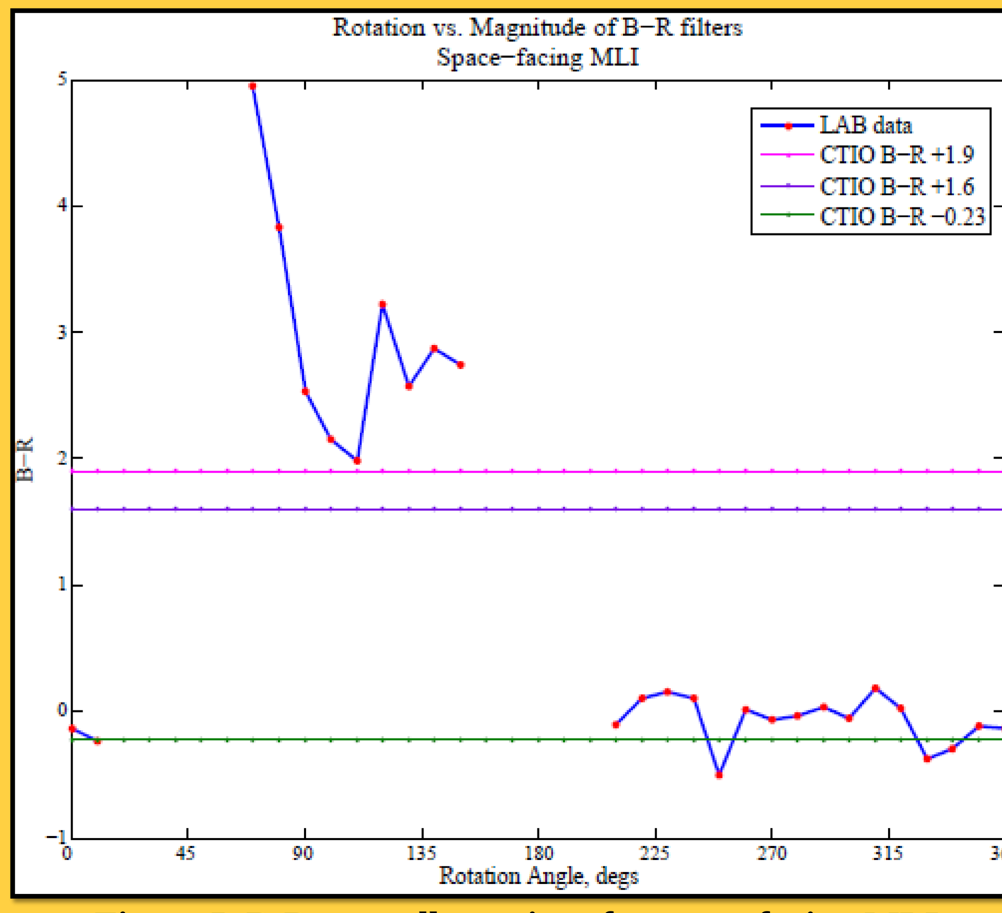

Figure 5. B-R over all rotations for space-facing MLI (copper-colored Kapton illuminated first, followed by aluminized Kapton) over plotted with telescopic B-R.

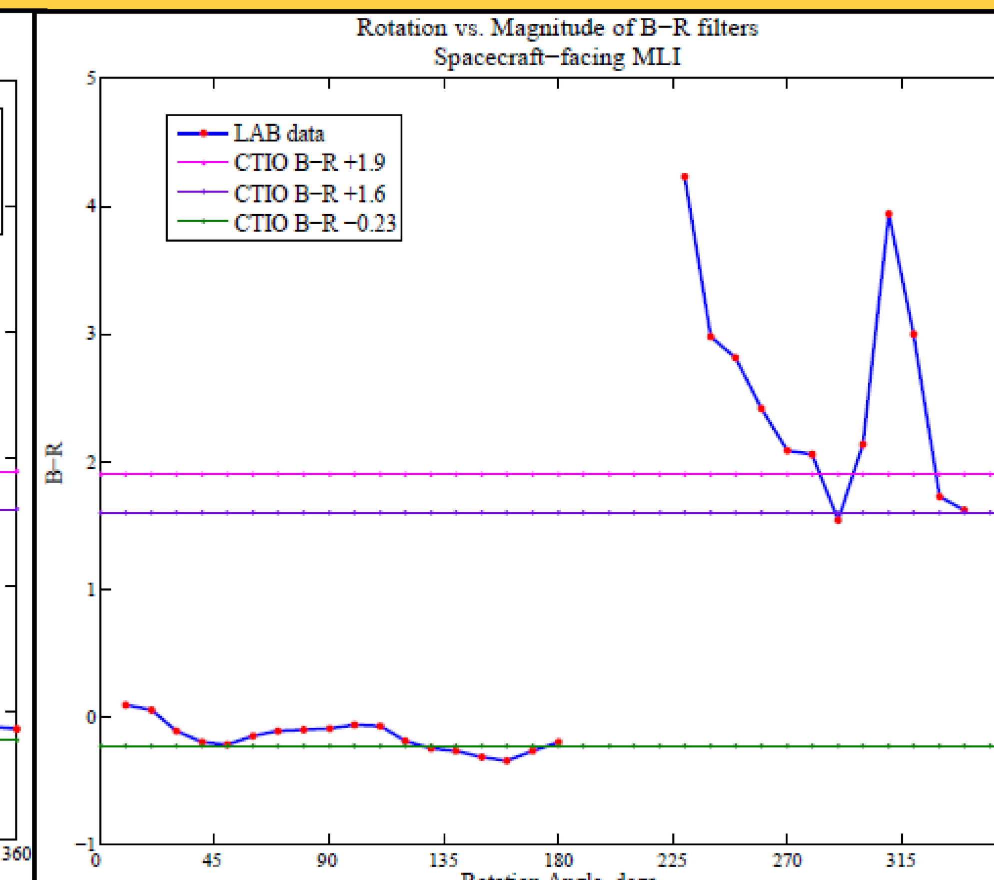

Figure 6. B-R over all rotations for spacecraft-facing MLI (aluminized Kapton illuminated first, followed by copper-colored Kapton) over plotted with telescopic B-R.

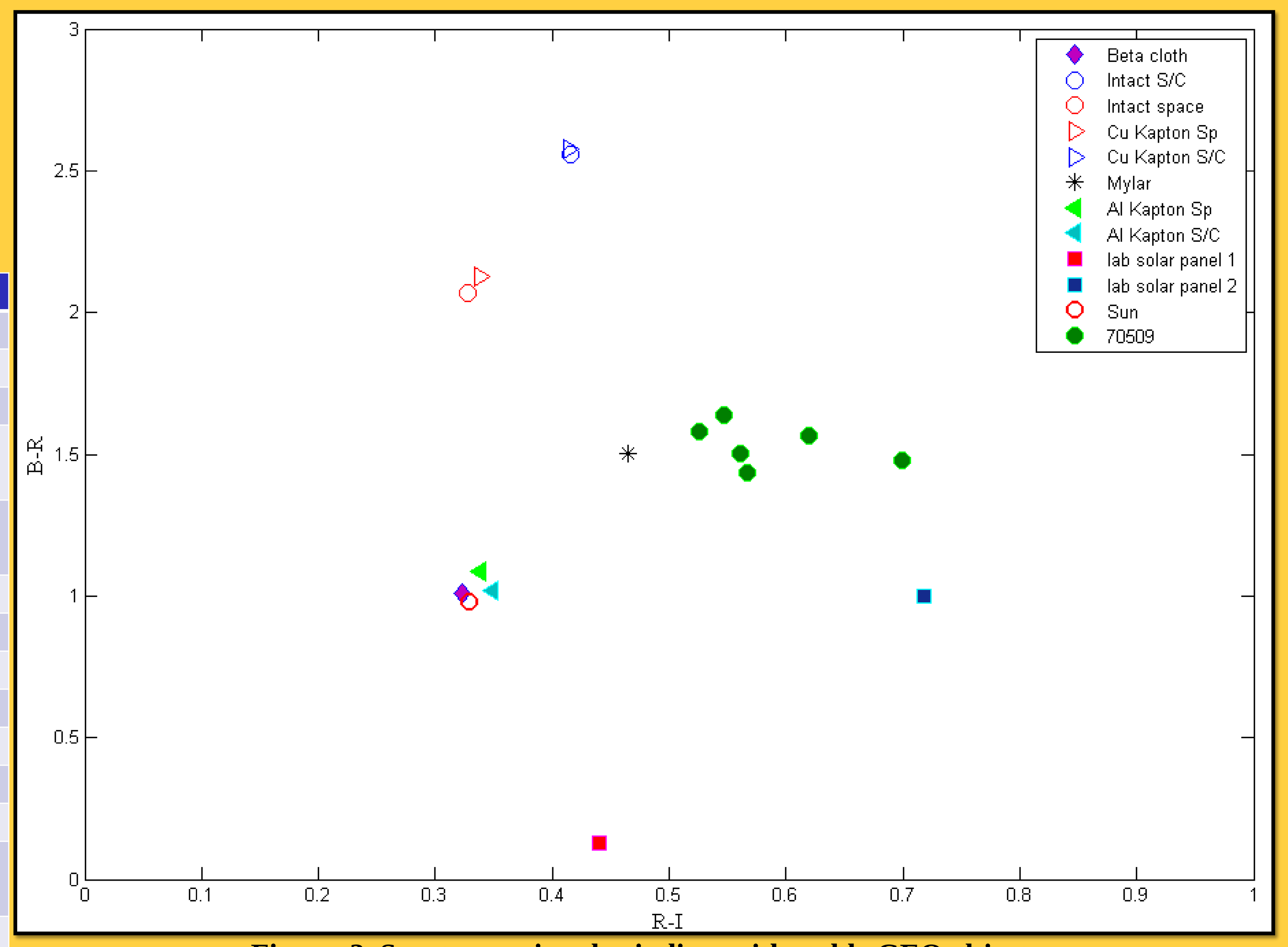

Figure 3. Spectroscopic color indices with stable GEO object.

Conclusions

- Color index data relative to the blue filter were presented for all objects.
- Materials with low signal return in the I band, require an increase in exposures without saturation and increase in SNR by co-adding more images to bring up the signal and decrease the image noise. This procedure will be used for future work to maximize the best return for all materials in each filter.
- Majority of the photometric color indices for the 14 fragments were near solar colors, whereas the copper Kapton colors showed magnitudes much redder than the sun.
- The JPL solar panel also showed close proximity to the copper Kapton material in the color index plots using only the photometric data. Unlike the spectral data, which only concentrated on the solar cell material, the JPL solar panel was found to be much bluer than the sun.
- Correlations to telescopic data must focus on objects that have a stable brightness over the measurement period; otherwise the scatter in the magnitude plots due to flashers/glints makes correlations impossible. One of the stable objects investigated showed a close proximity to Mylar and solar panel.
- Another object investigated using the CTIO 0.9 m showed a dramatic magnitude change, over nearly 2 hours increasing signal in the blue and visible filter, but decreasing shortly after in the red and infrared filters. This type of color change was consistent with laboratory measurements of the MLI layers when the aluminized Kapton layers become illuminated.

References

1. Cowardin, H., et al, An Assessment of GEO Orbital Debris Photometric Properties Derived from Laboratory-Based Measurements, 2009 AMOS Technical Conference Proceedings, Kihei, Maui, HI, 2009.
2. Cowardin, H., *Characterization of Orbital Debris Objects over Optical Wavelengths via Laboratory Measurements*, PhD thesis, Houston, TX, May 2010.